

Spatial and Temporal Assessment of Vegetation Cover in Al- Suwaiq Using Satellite Images Analysis

Kathiya Al-Aufi¹, Malik Al-Wardy^{1*}, Bheemanagoud Choudri², Mushtaque Ahmed¹, Ghazi Al-Rawas³, Yaseen Al-Mulla¹

التقييم المكاني والزمني للغطاء النباتي في ولاية السويق وتحليله باستخدام صور الأقمار الصناعية

كاذية العوفي^١ ومالك الوردى^{١*} وبيماناغود تشودري^٢ ومشتاق أحمد^١ وغازي الرواس^٣ وياسين الملا^١

ABSTRACT. Digital change detection techniques using multi-temporal satellite imagery help in understanding landscape dynamics. This study assesses the spatial and temporal dynamics of vegetation cover change in the coastal wilayat of Al-Suwaiq, Sultanate of Oman, using field and remote sensing data. The study was conducted at selected distances from the coastline, considering the variability in soil and water salinity. Normalized Difference Vegetation Index was calculated using the Landsat 5 TM and Landsat 8 OLI satellite images and classified into three main classes to evaluate the monthly and annual vegetation cover change between 1987 and 2016. Soil and water samples were collected during the cultivated season in Al-Suwaiq and analyzed mainly for salinity. Vegetation cover maps showed a general shift in vegetation biomass from regions closer to the coast (north-side) as water salinity increased with time. Between 1988 and 1999, vegetation cover in the total study area increased by 7.7%, whereas it declined by 1.5 % along the coast. However, between 1999 and 2016, the vegetation cover decreased further by 5% along the coast while increasing by 12.2%, mainly 3-6 km from the coast. The largest increase in the area was for vegetation covers falling within the moderate (0.33-0.67) and high (0.67-0.86) NDVI classes. In conclusion, vegetation cover in Al-Suwaiq reduced along the coastline and shifted agriculture activities and increased cultivation from the North to the South of Wilayat. Therefore, agriculture activities on the Southside of the Wilayat should be controlled to prevent further degradation of water quality and its possible effect on agricultural farmlands.

KEYWORDS: Landsat; NDVI; Vegetation cover; Change detection; Al-Suwaiq; Soil salinity; Water salinity.

المستخلص: تلعب صور الأقمار الصناعية والتقنيات الرقمية المتصلة بها دوراً مهماً في فهم ديناميكية التغير في الغطاء النباتي على الأرض. وتقييم هذه الدراسة الديناميات المكانية والزمانية لتغير الغطاء النباتي في ولاية السويق في سلطنة عمان باستخدام البيانات الميدانية وبيانات الاستشعار عن بعد. وأجريت هذه الدراسة على مسافات محددة من الساحل آخذةً في الاعتبار التباين الموجود في ملوحة التربة والمياه في منطقة الدراسة، حيث تم حساب مؤشر التغير للغطاء النباتي باستخدام صور القمر الصناعي لاندسات ٥ والقمر لاندسات ٨، ومن ثم تصنيف الغطاء النباتي إلى ثلاث فئات رئيسية لتقييم التغير الشهري والسنوي في الغطاء النباتي بين عامي ١٩٨٧ و ٢٠١٦. وتم أيضاً جمع عينات من التربة والمياه من المزارع التي تقع في منطقة الدراسة في ولاية السويق وتحليل معايير الملوحة فيها. وأظهرت خرائط الغطاء النباتي تغيراً عاماً في الكتلة الحيوية للغطاء النباتي في المناطق القريبة من الساحل (شمال منطقة الدراسة) بسبب تملح المياه مع مرور الوقت وتحولها إلى الجهة الجنوبية، حيث زادت مساحة الغطاء النباتي الإجمالية في منطقة الدراسة بين عامي ١٩٨٨ و ١٩٩٩ بنسبة ٧,٧٪، بينما انخفضت هذه النسبة بمقدار ١,٥٪ على طول الساحل في نفس الفترة، وزادت نسبة الإنخفاض هذه على طول الساحل إضافياً في الفترة ما بين عامي ١٩٩٩ و ٢٠١٦ بمقدار ٥٪، بينما زادت هذه النسبة من مساحة الغطاء النباتي بشكل إضافي وفي نفس الفترة بمقدار ١٢,٢٪ على مسافة ٣-٦ كيلومتر من الساحل. وكانت الزيادة الأكبر في المساحة هي للغطاء النباتي الواقع ضمن فئتين لمؤشر التغير للغطاء النباتي وهما المعتدلة (٠,٣٣-٠,٦٧) والعالية (٠,٦٧-٠,٨٦). وفي الختام خلصت الدراسة إلى تقلص الغطاء النباتي على طول الساحل في ولاية السويق وتحولت الأنشطة والرعي الزراعية من شمال منطقة الدراسة إلى جنوبها، ولذلك وجب مراقبة الأنشطة الزراعية الواقعة في الجهة الجنوبية لمنع المزيد من التدهور في جودة المياه وتأثيرها المحتمل على الأراضي الزراعية.

الكلمات المفتاحية: لاندسات، مؤشر التغير للغطاء النباتي، الغطاء النباتي، كشف التغير، السويق، ملوحة التربة، ملوحة المياه

Introduction

The detection of vegetation cover change can help for a better understanding of the interactions between humans and the ecosystem (Aly et al., 2016). According to Purevdorj et al. (1998), vegetation

Malik Al-Wardy^{1*}  mwardy@squ.edu.om, ¹Department of Soils, Water, and Agricultural Engineering, College of Agricultural and Marine Sciences, Sultan Qaboos University, Muscat, Oman. ²Center for Environmental Studies and Research, Sultan Qaboos University, Muscat, Oman. ³Department of Civil and Architectural Engineering, College of Engineering, Sultan Qaboos University, Muscat, Oman.

cover can be used as an indicator of land degradation and desertification in arid and semi-arid lands. Furthermore, the estimation of vegetation cover is essential for livestock breeding, agriculture, and helping land managers to minimize the danger of soil salinization (Wiegand et al., 1994).

Spatial and temporal changes in vegetation cover can be effectively and rapidly observed by remote sensing techniques using different vegetation indices (Alhammadi and Glenn, 2008). Vegetation indices (VI) determine vegetation cover by collecting useful information about



the vegetation such as the vegetation health, vegetation abundance, vegetation type, and growing conditions under various environments, e.g., soil salinity (Zhang et al., 2011). These indices describe the vegetation cover based on the amount of reflectance in the near-infrared band (NIR) and visible red band (R) regions of the electromagnetic spectrum. Many studies showed that the Normalized Difference Vegetation Index (NDVI) was the most popular index among operational users of remote sensing data because of the complexity of other indices (Rondeaux et al., 1996). Vegetation indices are used at all scales ranging from small local projects to global investigation (Walthall et al., 2004). The Normalized Difference Vegetation Index is the most commonly used index to map spatial and temporal variation in vegetation (Tucker, 1979), and it is the best index for a wide range of vegetation densities (Purevdorj et al., 1998). It has been used extensively to describe the different vegetation properties, like the amount of green cover, biomass production, green leaf area, and productivity (Alhammadi and Glenn, 2008). Normalized Difference Vegetation Index values range between -1.0 and 1.0, where values of zero and below indicate the presence of water, snow, ice, or clouds. In contrast, values above 0 indicate the presence of vegetation at different densities. Normalized Difference Vegetation Index values close to 1 (0.8 - 0.9) indicate high vegetation density (Fu and Burgher, 2015). When plants grow under stress like high soil salinity, it causes reduction in chlorophyll and damage to plant cell structure. This causes a decrease in near infrared reflectance and increase in visible reflectance (Dunagan et al., 2007). These differences in reflectance in the two bands give valuable information about vegetation health and cover change due to various environmental stresses.

In this study, Landsat satellite images for the coastal Wilayat of Al-Suwaiq in the North Al-Batinah Governorate of Oman were used to assess the monthly and annual vegetation cover change with the help of the NDVI index for the period from 1987 to 2016. Vegetation health and biomass were evaluated for regions related to their distance from the coastline and soil and water salinity.

Study Area

This study was carried out in the coastal plains of Wilayat Al-Suwaiq (23°50'58"N 57°26'19"E), located in Al-Batinah North Governorate in the Northern part of Oman (Figure 1). According to PACA (2020), the mean annual rainfall in Al-Suwaiq is 109 mm, with the months of December-March being the wettest and the months of May-September being the driest. The mean yearly maximum temperature is 34°C, with a daily maximum exceeding 49 °C during the summer months, while the mean minimum annual temperature is 22°C. Al-Suwaiq covers an area of approximately 1,000 km² with a total cultivated land of 80 km². Moreover, a study was done by Choudri et al., (2015) and found that Al-Suwaiq had

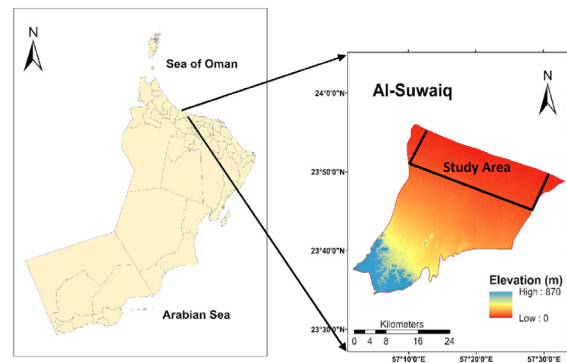


Figure 1. Location map of Wilayat Al-Suwaiq in North Al-Batinah Governorate, Oman

the highest population density and intensive agriculture in Al-Batinah North consuming the largest amount of groundwater, which typically is the primary source of irrigation water. The most popular crops in Al-Suwaiq are squash, Rhodes grass, banana, date palm, alfalfa, and tomato (Al-Aufi et al., 2020). The agricultural season in the study area starts from October to April as it has a direct relation with temperature and rainfall patterns. The main rainfall season in northern Oman is between December and April (MAF and ICBA, 2012).

Materials and Methods

Satellite Images Data

Cloud-free Landsat 5 TM (Thematic Mapper) and Landsat 8 OLI (Operational Land Imager) satellite images for Al-Suwaiq were downloaded from the USGS Earth Explorer website. In general, Landsat 5 has six reflective bands, while Landsat 8 has nine. Both have bands with a spatial resolution of 30 m in the visible and near-infrared regions of the electromagnetic spectrum; however, the spectral resolution of the red and infrared bands of Landsat 8 is narrower. Table 1 shows the sensor characteristics of both satellites.

Landsat 8 (OLI) images for the 12 months of the year 2015 were used to determine the growing season in the study area. In addition, a first-order harmonic model with a linear regression reducer was fit to a time series of Landsat 8 (OLI) NDVI images for the years 2013 to 2016 using the Google Earth Engine® platform. This allowed us to determine the months with peak agriculture activity in Al-Suwaiq, and hence, to determine the best month to be used for the annual changes detection. Table 2 provides details of the selected images used to detect the monthly change in vegetation biomass during the growing season in the study area from 1987 to 2016.

Table 1. Sensor characteristics of Landsat 5 (TM) and Landsat 8 (OLI) satellites

Satellite/ Sensor	Band Number	Band Name	Spectral Range (µm)	Spatial Resolution (m)	Radiometric Resolution	Repeat Cycle (Days)
Landsat 5 (TM)	1	Blue	0.45 - 0.52	30	8 bits	16
	2	Green	0.52 - 0.60	30		
	3	Red	0.63 - 0.69	30		
	4	Near-Infrared	0.76 - 0.90	30		
	5	Shortwave Infrared 1	1.55 - 1.75	30		
	6	Thermal Infrared	10.40 - 12.50	120		
	7	Shortwave Infrared 2	2.08 - 2.35	30		
Landsat 8 (OLI)	1	Coastal Aerosol	0.43 - 0.45	30	12 scaled to 16	16
	2	Blue	0.45 - 0.51	30		
	3	Green	0.53 - 0.59	30		
	4	Red	0.64 - 0.67	30		
	5	Near-Infrared	0.85 - 0.88	30		
	6	Shortwave Infrared 1	1.57 - 1.65	30		
	7	Shortwave Infrared 2	2.11 - 2.29	30		
	8	Panchromatic	0.50 - 0.68	15		
	9	Cirrus	1.36 - 1.38	30		
	10	Thermal Infrared 1	10.6 - 11.19	100		
	11	Thermal Infrared 2	11.5 - 12.51	100		

Source: <https://landsat.gsfc.nasa.gov/>

Image Preprocessing

Image preprocessing is a crucial step to improve image quality and increase accuracy (Munyati, 2000). The image preprocessing includes geometric and atmospheric corrections that reduce and eliminates errors. Image geometric correction is the process of precisely matching the image's projection to a specific projection surface or shape (Hyypa et al., 2000). The downloaded images were geo-rectified to the Universal Transverse Mercator (UTM) coordinate system with the datum World Geodetic System (WGS) 1984 and zone 40 north.

The atmosphere, on the other hand, can have a critical impact on the electromagnetic energy sensed by the imaging system detectors (Chavez, 1996), changing its spectral distribution and introducing some skylight into the sensor field-of-view (Gilbert et al., 1994). These images were atmospherically corrected to convert digital number values into surface reflectance using the ATCOR ground reflectance workflow in the PCI Geomatica® software.

Vegetation Cover Measurement

The vegetation cover change was evaluated using the Normalized Difference Vegetation Index (NDVI), which utilizes the red and near-infrared wavelengths to generate single-band images (Tucker, 1979)

$$NDVI = (NIR-RED) / (NIR+RED) \quad (1)$$

The threshold for separating vegetation from non-vegetation was carefully determined with the aid of high-resolution images from Google Earth® and ground truth information. After careful examination and based on Holben (1986), vegetation cover based on NDVI values were divided into three classes (Table 3).

Vegetation Change Detection

Change detection is defined as the process of identifying differences in the state of an object by quantifying temporal effects (Singh, 1989). According to Singh (1989), change detection can be used for various purposes such as land utilization analysis, vegetation cover change, observing deforestation, crop diseases, stress detection, and disaster monitoring.

The temporal changes in vegetation were detected and quantified using the raster calculator in ArcMap® 10.1. The classified NDVI raster images produced in the previous step for the years 1988, 1999, and 2016, the month of February (Table 2), were subtracted consecutively to detect and quantify spatial vegetation changes between these periods.

Vegetation Cover Change with Distance from the Coastline

According to (MAF and ICBA, 2012), between 1994 and 2004, there was a significant change in groundwater electric conductivity (EC) in the monitoring wells locat-

Table 2. Monthly Landsat 8 (OLI) images used for monthly detection change

Image	Year	Day/Month	Satellite	Path	Row
1	1987	8-October	Landsat 5(TM)	159	43
2	1987	28-December	Landsat 5(TM)	158	44
3	1988	5-February	Landsat 5(TM)	159	43
4	1988	1-March	Landsat 5(TM)	158	44
5	1994	20-October	Landsat 5(TM)	158	44
6	1994	7-December	Landsat 5(TM)	158	44
7	1995	16-February	Landsat 5(TM)	159	43
8	1995	29-March	Landsat 5(TM)	158	44
9	1996	16-October	Landsat 5(TM)	159	43
10	1996	19-December	Landsat 5(TM)	159	43
11	1997	21-February	Landsat 5(TM)	159	43
12	1997	2-March	Landsat 5(TM)	158	44
13	1998	22-October	Landsat 5(TM)	159	43
14	1998	2-December	Landsat 5(TM)	158	44
15	1999	20-February	Landsat 5(TM)	158	44
16	1999	31-March	Landsat 5(TM)	159	43
17	2014	18-October	Landsat 8 (OLI)	159	43
18	2014	5-December	Landsat 8 (OLI)	159	43
19	2015	16-February	Landsat 8 (OLI)	158	44
20	2015	4-March	Landsat 8 (OLI)	158	44
21	2015	5-October	Landsat 8 (OLI)	159	43
22	2015	24-December	Landsat 8 (OLI)	159	43
23	2016	19-February	Landsat 8 (OLI)	158	44
24	2016	13-March	Landsat 8 (OLI)	159	43

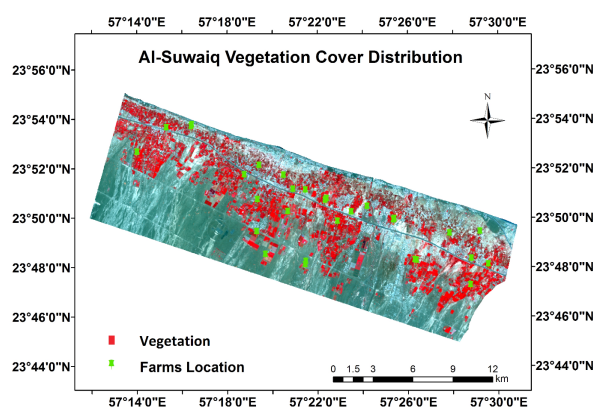
Source: <https://earthexplorer.usgs.gov/>

ed approximately 5 km from the coastal area of Al-Batinah. Therefore, the study area was divided into two distance from coastline classes to monitor and quantify the temporal vegetation cover changes with this distance. A buffer tool in ArcMap® 10.1 was utilized to divide the area into a 0-3 km (North) and 3-6 km (South) distance from the coastline.

Soil and Water Sampling and Laboratory Analysis

Soil and water samples were collected during the cultivated season in Al-Suwaiq in March 2016. Sixty soil samples were collected randomly from 30 different farm locations making sure the samples uniformly cover the study area from the coast to 9 km inland (~ 23,361 hectares) (Figure 2). During soil sampling, composite soil samples comprised of three subsamples of surface (0-10cm deep) and subsurface (10-20 cm deep) soils were collected in each farm location. Groundwater samples were collected from 36 wells located in the same fields where the soil samples were collected.

Soil and water samples were transferred to the laboratory where the soil was dried and sieved. The soil pH and electrical conductivity were measured from a saturated


Figure 2. Soil and water sampling sites.

soil paste. The soil texture was determined using the hydrometer method based on Stoke's law, which states that particles of different sizes will settle out of suspension at different rates over time (Bouyoucos, 1962).

Water pH and electrical conductivity were measured directly in the solution. The sodicity of water, which

Table 3. Vegetation classes based on NDVI

NDVI	Class
0.21 – 0.33	low green-leaf-vegetation
0.33 – 0.67	moderate green-leaf-vegetation
0.67 – 1.00	high green-leaf-vegetation

promotes soil dispersion and causes reduced hydraulic conductivity and aeration, was determined by analyzing for Na^+ , Ca^{2+} , and Mg^{2+} (expressed in meq/L) in water and calculating the sodium adsorption ratio (SAR) as follows:

$$\text{SAR} = \text{Na} / \sqrt{[(\text{Ca} + \text{Mg}) / 2]} \quad (2)$$

Spatial Interpolation

Spatial interpolation is extensively used in soil sciences to estimate the spatial pattern of various soil chemical properties. According to (Omran, 2012; Mehdi et al., 2013; Bhunia et al., 2018), the kriging interpolation, which takes into consideration the spatial autocorrelation of the measured sampled points with distance, is the best method to estimate the spatial distribution of soil organic carbon, soil EC, and soil pH.

In this study, ordinary kriging was used to map the pattern of soil and water salinity in the area. Spherical, exponential, and Gaussian models were used to fit the log-normally distributed soil and water EC data. The Gaussian model was found to have the smallest root mean square error, and, hence, was used to predict soil and water salinity distribution. Although the number of samples was relatively small for a smooth spatial interpolation, the samples were well distributed, and studies have shown that ordinary kriging can perform well for interpolating soil properties when the number of data is limited (Schloeder et al., 2001). A complete flowchart routine of methodology used is illustrated in Figure 3.

Results and Discussion

Soil Analysis

The overall soil texture analysis in the study area indicated that 27% of soils are sand and loamy sand, 35% are sandy loam, 30% are silt loam and loam, and only 8% are either silty clay, silty clay loam, sandy clay loam, or clay loam. Generally, the soil texture in the study area is coarse to moderately coarse, which means the soils have high water drainage and very low nutrient and water holding capacity (MAF and ICBA, 2012).

Table 4 shows the analysis results of soil samples collected from the farms. The Food and Agriculture Organization (FAO) classifies soils with EC values greater than 2 dS/m as considered saline (Abrol et al., 1988). According to the FAO soil salinity classification, 17% of the surface soils in the agricultural farms of the study are

Table 4. Soil salinity and pH in surface and subsurface soils

Soil depth	EC (dS/m)			pH		
	Mean	Max	Min	Mean	Max	Min
Surface (0-10 cm)	7.35	34.90	0.84	7.70	8.10	6.90
Subsurface (10-20 cm)	5.16	20.10	1.09	7.63	8.10	7.00

classified as non-saline (0-2 dS/m), 38% as slightly saline, 18% as moderately saline (4-8 dS/m), 16% as strongly saline (8-16 dS/m), and 11% as very strongly saline (>16 dS/m).

Spatial interpolation of soil salinity shows that surface and subsurface soil salinity is higher in the agricultural farms closer to the coastline (Figures 4 and 5). This was very much related to the irrigation water quality, as it can be seen from the groundwater salinity maps. Intensive agricultural activities closer to the coastline resulted in excessive groundwater pumping leading to intrusion and the salinization of groundwater (Zekri, 2008). The majority of farms farther from the coastline are non-saline to slightly saline (< 4 dS/m). Additionally, surface soils were found to be more saline than subsurface soils as a result of salt accumulation at the surface as the irrigation water evaporates (Sommerfeldt and Rapp, 1982).

Non-saline to slightly saline surface soils covered 63% of the mapped agricultural land in the study area. In comparison, 30% of the area was moderately saline, 7% was strongly saline, and only 1% of agricultural land was very strongly saline. On the other hand, non-saline to slightly saline subsurface soils covered 76% of the agricultural land in the study area, while 19.2% was moderately saline, 3.6 % was strongly saline, and only 0.3% was very strongly saline.

Water Analysis

Table 5 shows the analysis results of groundwater samples collected from the wells in the farms. According to the FAO water salinity classification (Rhoades et al., 1992), 3% of water samples were non-saline (< 0.7 dS/m), 54% were slightly saline (0.7 – 2.0 dS/m), 37% were moderately saline (2 – 10 dS/m), and 6% were highly saline (10 – 25 dS/m). The sodium hazard of the groundwater used for irrigation was very low as the maximum SAR value was 2.1. This means the irrigation water in the study area, although saline, does not have any potential to cause soil dispersion and infiltration problems and to

Table 5. Main chemical properties of groundwater in the study area

Water properties	Mean	Max	Min
EC (dS/m)	3.20	19.52	0.50
pH	7.82	8.4	7.0
SAR	1.10	2.10	0.73

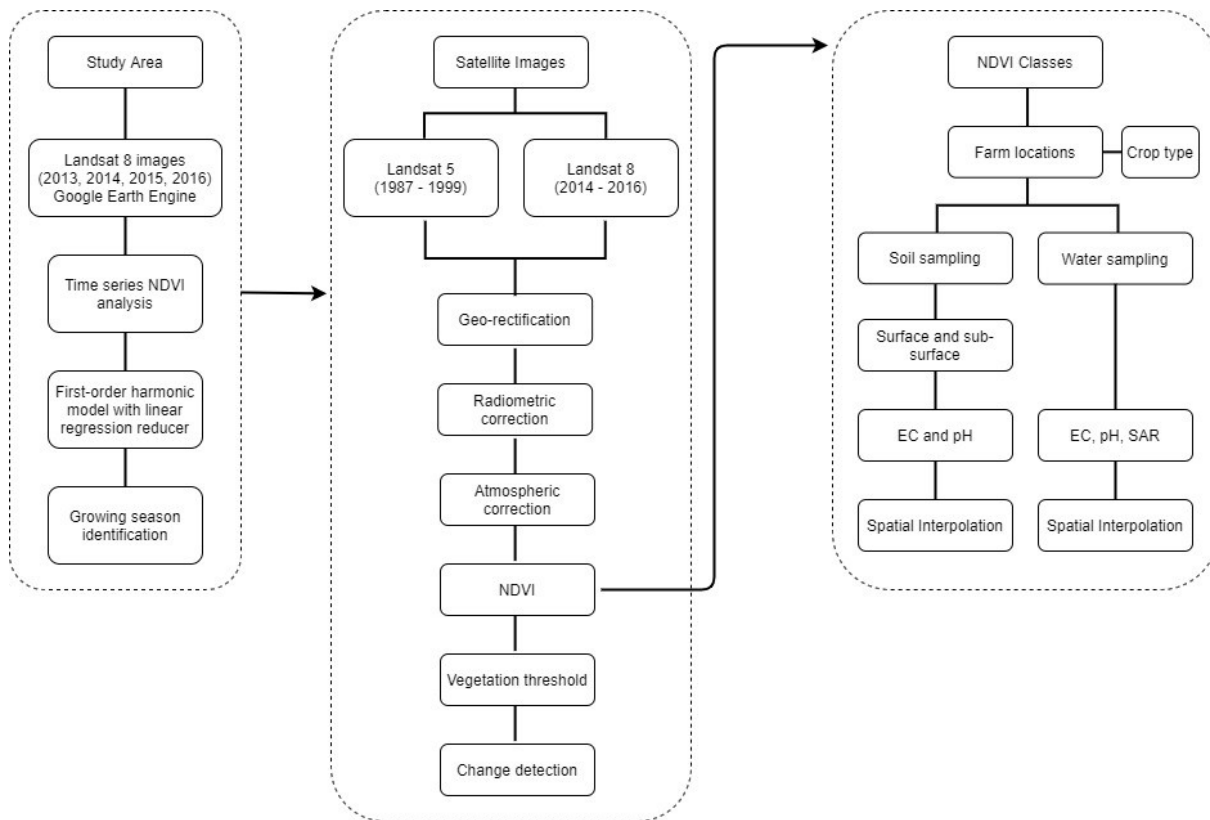


Figure 3. Flowchart of methodology

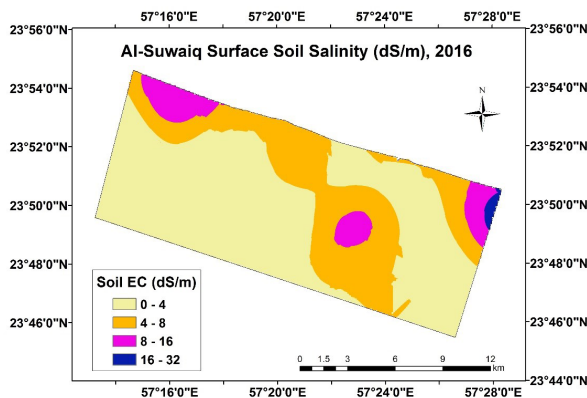


Figure 4. The pattern of soil salinity in surface soils.

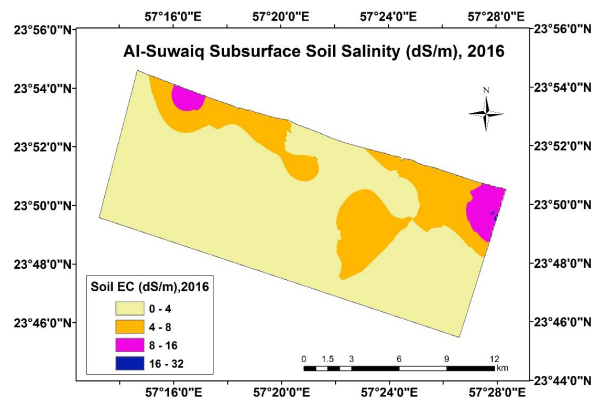


Figure 5. The pattern of soil salinity in subsurface soils.

aggravate the soil salinity problem further.

Spatial interpolation of water salinity showed most of the groundwater in the study area closer to the coastline ranges from moderately to highly saline (Figure 6). According to data collected by the Ministry of Regional Municipalities and Water Resources from monitoring wells, non-saline groundwater covered about 3.4% of the study area in 2010. This area, according to this study, was reduced to 0.8% in 2016. Slightly saline and highly saline

were also slightly reduced from 67% to 64% and 2.6% to 2.2%, respectively. The moderately saline groundwater area increased from 27% to 33% of the study area.

Satellite Images Selection for Vegetation Cover Change Analysis

The vegetation cover in the study area is very heterogeneous, including trees, shrubs, and grass of various species. Therefore, vegetation separation based on their

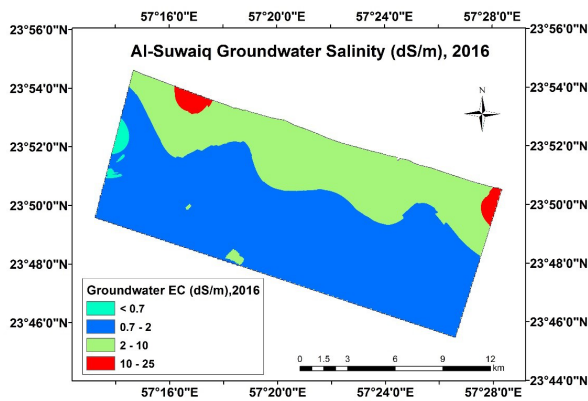


Figure 6. The pattern of groundwater salinity in the study area.

spectral characteristics using medium resolution satellite images from the Landsat mission becomes more complex and very difficult (Xiao and McPherson, 2005). Hence, a threshold for separating vegetation from non-vegetation was carefully determined with the aid of high-resolution images from Google Earth® and ground truth information to be around an NDVI value of 0.21.

The best period within the year to study vegetation cover in the study area using NDVI was identified using satellite images for the twelve months of the year 2015. Maximum NDVI, mean above 0 and mean above 0.21, were plotted (Figure 7) and showed that the highest mean and maximum NDVI values occurred in January, while the lowest were in July. As the type of vegetation cover varies in the study area. Therefore, a first-order harmonic model was fit to a time series of Landsat 8 (OLI) NDVI images for the years 2013 to 2016 (Figure 8) to smooth the seasonal variations in NDVI values and

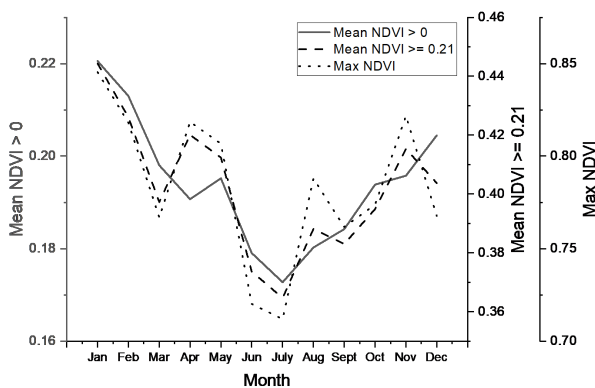


Figure 7. Maximum, mean above zero, and mean above 0.21 NDVI values for the twelve months of the year 2015

produce a unimodal seasonal pattern. It was observed that the low NDVI values occurred towards the end of the growing season during the dry and hot periods (June-September), and the high NDVI values occurred during the rainy and cooler period (December-March). The maximum values (amplitude) according to the fitted model were mainly in the month of February, and the midpoints between the highest and lowest values were in the months of October and March. According to these results, NDVI values for the growing season from October to March were calculated for the different years and compared, while the month of February was used as the base month for change detection.

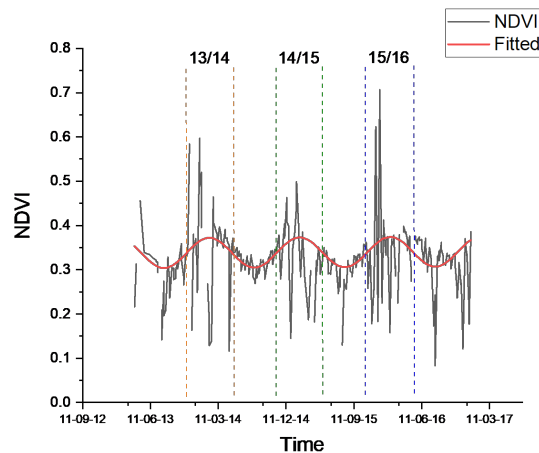


Figure 8. Actual and first harmonic fitted NDVI values for the years 2013 to 2016

Vegetation Cover Change – Temporal

In general, vegetation cover has significantly changed in North and South Al-Batinah Governorates since the 1980s. Satellite images for the study area showed that the mean NDVI values during the growing season from October to March have increased from 0.29 in 1988 to 0.38 in 2016 (Figure 9). This increase in the mean NDVI was mainly due to the increase in the total cropped area (Figures 10, 11, and 12). According to the Agricultural census carried out by the Ministry of Agriculture and Fisheries, the total cropped area in the whole Wilayat Al-Suwaiq increased from 5835 ha in 1993 to 5887 ha and 11460 ha in 2005 and 2013, respectively (MAF, 1993; 2005; 2013). Moreover, the cropping pattern has considerably changed during this period. There was a sharp increase in the cropped area of Rhodesgrass and Squash from 2005 to 2013. The total cropped area increased from about 1080 ha to 2500 ha and from 38 ha to 4315 ha for Rhodesgrass and Squash, respectively (Al-Aufi, et al. 2020). However, there was a decrease in the cropped area for the same period for Date palms and alfalfa from 1865 ha to 1222 ha and 372 ha to 207 ha, respectively.

In addition, ground-truthing was carried out and showed that, in 2016, out of the 14 locations showing high NDVI values (0.67-0.86), 12 were growing Rhodes-grass and one each for banana trees and alfalfa. As for sites showing moderate NDVI values (0.33-0.67), 13 locations were visited where five were growing Rhodes-grass, and the rest was a mixture of vegetable and field crops with mango and date palm trees. The changes in the NDVI values for the Rhodesgrass between high and moderate might be attributed to various factors such as the growth stage, soil fertilization, or poor management. The lower NDVI (0.21-0.33) sites mainly represented native shrubs and trees and the invasive *Prosopis juliflora*; however, few of these sites were also found to grow vegetables on smaller scales.

The analysis of the different NDVI classes (Figure 13) in the study area showed that there was a slight increase in the pixel counts for the lower class of 0.21-0.33, and hence a small rise in the vegetation area covered by this class. The vegetation cover area for the lowest class increased from 1861 ha in 1988 to 2915 ha and 2755 ha, for the years 1999 and 2016, respectively (Table 6). The mean NDVI value, however, remained constant at around 0.26. The pixel counts for the middle class of 0.33-0.67 has increased considerably across the class range from 1988 to 2016, and the vegetation cover area increased more than six folds from 725 ha in 1988 to 4565 ha in 2016. The mean NDVI value has also increased from 0.40 to 0.48 for the same period of the middle class. The largest increase in pixel counts, and hence vegetation cover area,

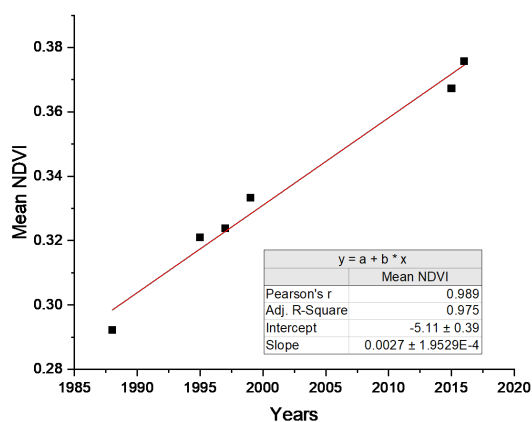


Figure 9. Mean NDVI during the growing season from 1988 to 2016

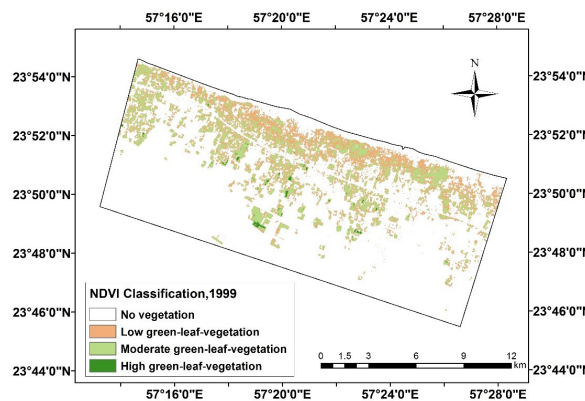


Figure 11. Vegetation cover classification in February 1999

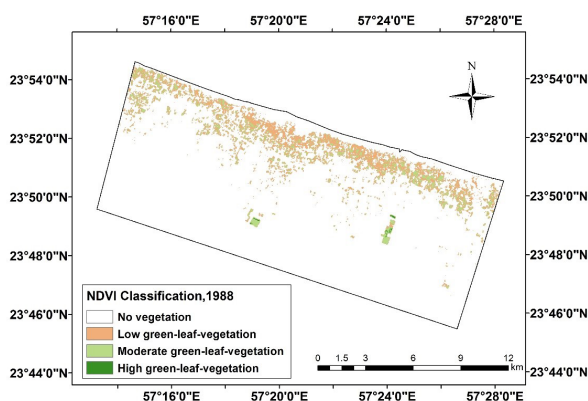


Figure 10. Vegetation cover classification in February 1988

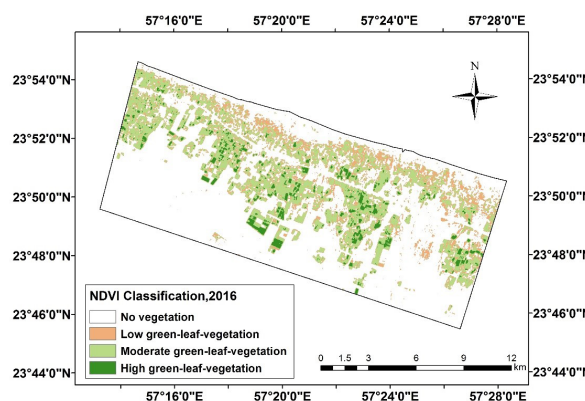


Figure 12. Vegetation cover classification in February 2016

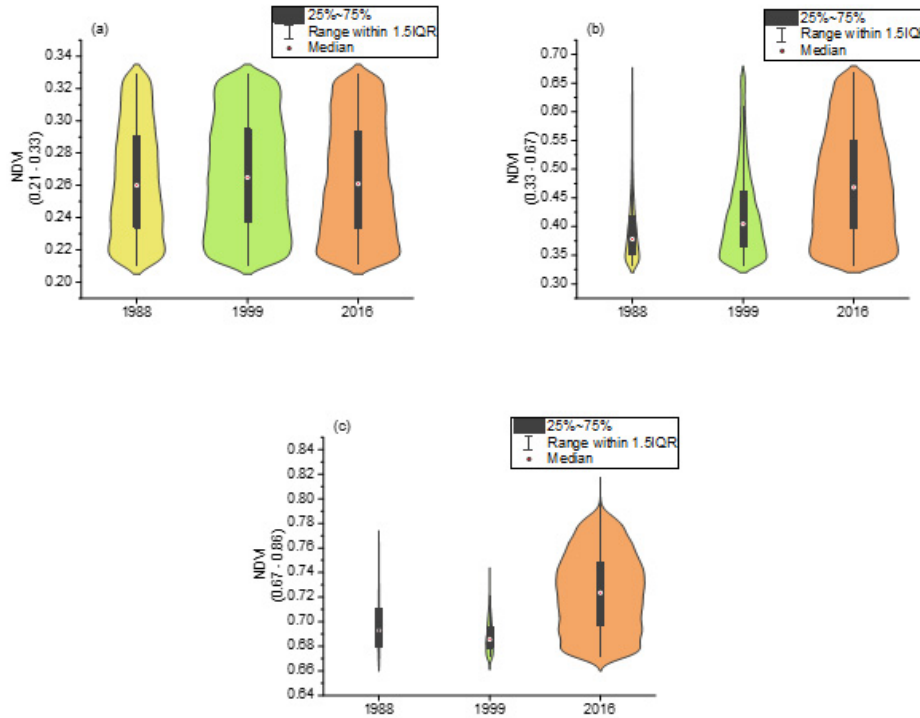


Figure 13. Figure 13. The difference in pixel counts of the three NDVI classes, (a) 0.21-0.33, (b) 0.33-0.67, (c) 0.67-0.86, from 1988 to 2016. The spread of this data set is described by the first and third quartiles, the median, and the 1.5*interquartile range (IQR).

was for the highest class of 0.67-0.86 and for the whole class range. The vegetation cover area had increased 72 folds from a mere 10 ha in 1988 to 719 ha in 2016.

This shows that with the advent of technology, there was a large expansion in agricultural activities and the cultivated area. The use of modern irrigation systems in Al-Suwaiq has increased to 78% in the year 2013 (Al-Aufi et al., 2020). However, as it was noted from field visits to sites of high NDVI values being mainly cultivated with Rhodesgrass, the large surge in the middle and high classes means greater pressure on the water resources in the study area. Each hectare cultivated with Rhodesgrass can consume up to 48,000 cubic meters of water

per year (MAF, 2019). This can only exacerbate the sea-water intrusion problem, resulting in more salinization of groundwater and, as a result, a more substantial loss of agricultural farms closer to the coastline.

Vegetation Cover Change – Spatial

ArcMap® 10.1 was used to show the difference in spatial vegetation cover change in the study area between 1988 and 1999, and 1999 and 2016 NDVI images. This differencing allowed to identify the sites where a positive (increase) or a negative (decrease) change in vegetation cover occurred. Figures 14 and 15 show a site-specific positive and negative change. Most of the positive

Table 6. NDVI mean and median, and corresponding area, for each class during the study period

Class / NDVI	1988			1999			2016		
	0.21	0.33	0.67	0.21	0.33	0.67	0.21	0.33	0.67
	-	-	-	-	-	-	-	-	-
	0.33	0.67	0.86	0.33	0.67	0.86	0.33	0.67	0.86
Mean	0.26	0.40	0.70	0.27	0.42	0.69	0.26	0.48	0.72
Median	0.26	0.38	0.69	0.26	0.40	0.69	0.26	0.47	0.72
Area (ha)	1861	725	10	2915	2442	58	2755	4565	719

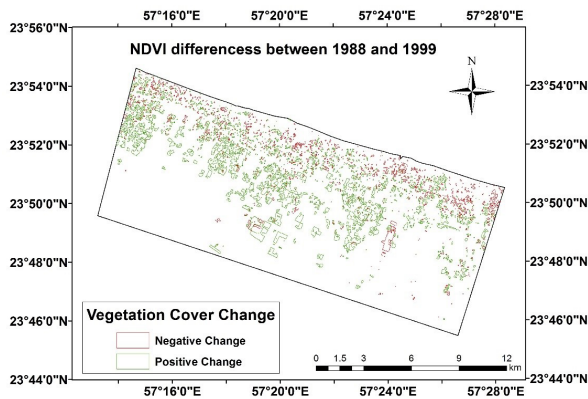


Figure 14. NDVI differences between February 1988 and February 1999

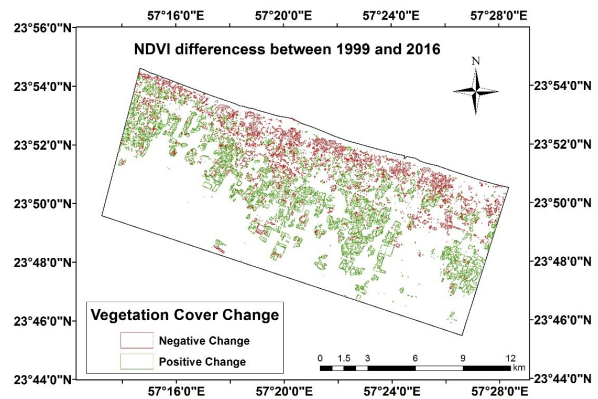


Figure 15. NDVI differences between February 1999 and February 2016

change in vegetation cover occurred farther from the coastline, whereas the negative change occurred closer to the coastline. However, in both periods, there was a more positive change in vegetation cover than negative. For the period between 1988 and 1999, there was an increase in vegetation cover by 1798 ha, mainly south of the main highway (3-6 km from the coastline), and a decrease of 350 ha north of the main highway closer to the coastline (0-3 km from the coastline). These losses in vegetation cover in 1999 account for about 14% of the total vegetation that was present in 1988. As for the period between 1999 and 2016, there was an additional increase in vegetation cover by 2843 ha and the reduction of an additional 1157 ha. These losses in vegetation cover in 2016 account for about 31% of the total vegetation that was present in 1999. The difference in vegetation cover area between 1988, 1999, and 2016 is summarized in Table 7.

Table 7. Change in vegetation cover in hectares and percentage of the total study area for the periods between 1988 – 1999, and 1999 - 2016

Class	1988 -1999		1999 -2016	
	Area(ha)	Percentage (%)	Area(ha)	Percentage (%)
Decrease in vegetation	350	1.5	1157	5.0
No change in vegetation	21212	90.8	19361	82.9
Increase in vegetation	1798	7.7	2843	12.2

The decline in the vegetation cover is mainly attributed to the deterioration in water quality. Figure 16 shows that most of the negative changes in vegetation cover occurred in areas that are affected by high groundwater salinity, mainly from 2 to 25 dS/m. This decline coincides

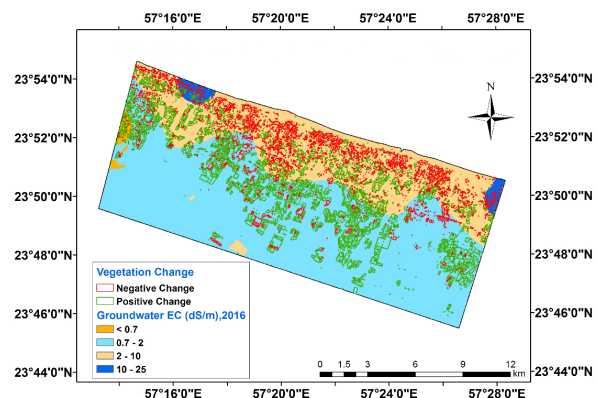


Figure 16. Vegetation cover change with water salinity

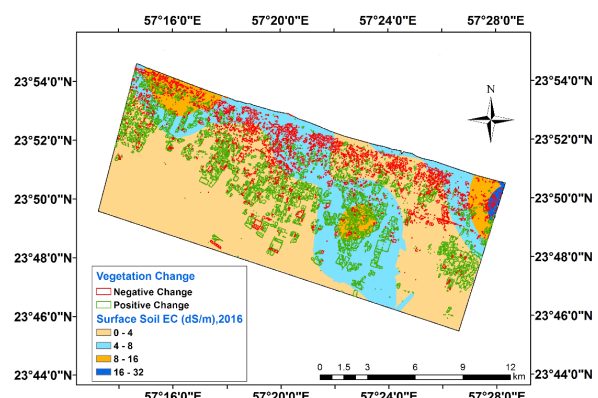


Figure 17. Vegetation cover change with soil salinity

mostly in the same areas with high surface soil salinity, between 4 and 32 dS/m (Figure 17). On the other hand, most positive changes, although varying in areas of different soil salinity, occurred in areas with low groundwater salinity, indicating the primary role played by the water quality in vegetation cover change rather than soil salinity.

Conclusion

Making use of remotely sensed available data to monitor spatial and temporal changes in the vegetation cover, especially in areas under environmental pressures such as soil and water salinity, allows for the sustainable management and planning of these lands. This study utilized the Landsat satellite images to perform vegetation cover analysis from 1988 to 2016 in Wilayat Al-Suwa'iq in North Al-Batinah Governorate using the Normalized Difference Vegetation Index in conjunction with field study in the years 2015 and 2016. The results showed that vegetation cover has significantly changed in the study area, increasing in the area from 2600 ha in 1988 to more than 8000 ha in 2016. This increase has mainly occurred farther (3-6 km) from the coastline, while areas closer to the coastline (0-3 km) have seen a decrease in vegetation cover. As the analysis has shown, 2.2 % and 33% of the study area is covered by highly and moderately saline groundwater, respectively, mainly existing closer to the coastline and must have impacted the vegetation cover in these areas negatively. This study also showed a surge in the vegetation cover falling within the moderate (0.33-0.67), and more importantly, the high class (0.67-0.86) NDVI values. This is indicative, according to field visits, of an increase in the cropped area of Rhodesgrass known for its high consumption of water, posing a great challenge for the future planning of the agricultural activities in the area and the management of water resources.

References

- Abrol IP, Yadav JSP, Massoud FI. (1988). Salt-affected soils and their management. FAO Soils Bulletin 39. Food and Agriculture Organization of the United Nations. Rome, Italy. 131pp.
- Al-Aufi K, Al-Wardy M, Choudri BS, Ahmed M. (2020). Analysis of agricultural cultivation trend: A shifting scenario in a coastal wilayat, Oman. *Environment, Development and Sustainability* 22: 2685-2698.
- Aly AA, Al-Omran AM, Sallam AS, Al-Wabel MI, Al-Shayaa MS. (2016). Vegetation cover change detection and assessment in arid environment using multi-temporal remote sensing images and ecosystem management approach. *Solid Earth* 7: 713-725.
- Alhammadi M, Glenn E. (2008). Detecting date palm trees health and vegetation greenness change on the eastern coast of the United Arab Emirates using SAVI. *International Journal of Remote Sensing* 29(6): 1745-1765.
- Bhunja GS, Shit PK, Maiti R. (2018). Comparison of GIS-based interpolation methods for spatial distribution of soil organic carbon (SOC). *Journal of the Saudi Society of Agricultural Sciences* 17(2): 114-126.
- Bouyoucos GJ. (1962). Hydrometer method improved for making particle size analysis of soils. *Agronomy Journal* 54:464-465.
- Chavez PS. (1996). Image-based atmospheric corrections-revisited and improved. *Photogrammetric Engineering and Remote Sensing* 62(9): 1025-1035.
- Choudri BS, Baawain M, Ahmed M, Al-Sidairi A, Al-Nadabi H. (2015). Relative vulnerability of coastal wilayats to development: a study of Al-Batinah North, Oman. *Journal of Coastal Conservation* 19(1): 51-57.
- Dunagan SC, Gilmore MS, Varekamp JC. (2007). Effects of mercury on visible/near infrared reflectance spectra of mustard spinach plants (*Brassica rapa* P.). *Environmental Pollution* 148(1): 301-311.
- Fu B, Burgher I. (2015). Riparian vegetation NDVI dynamics and its relationship with climate, surface water and groundwater. *Journal of Arid Environments* 113: 59-68.
- Gilbert M, Conese C, Maselli F. (1994). An atmospheric correction method for the automatic retrieval of surface reflectances from TM images. *International Journal of Remote Sensing* 15(10): 2065-2086.
- Holben BN. (1986). Characteristics of maximum-value composite images from temporal AVHRR data. *International Journal of Remote Sensing* 7(11): 1417-1434.
- Hyypä J, Hyypä H, Inkinen M, Engdahl M, Linko S, Zhu YH. (2000). Accuracy comparison of various remote sensing data sources in the retrieval of forest stand attributes. *Forest Ecology and Management* 128(1): 109-120.
- MAF. (1993). Agriculture census report. Oman: Ministry of Agriculture and Fisheries. 1992/1993
- MAF. (2005). Agriculture census report. Oman: Ministry of Agriculture and Fisheries. 2004/2005
- MAF. (2013). Agriculture census report. Oman: Ministry of Agriculture and Fisheries. 2012/2013
- MAF. (2019). <https://www.maf.gov.om/MediaCenter/NewsDetails/12663#> (accessed July 14,2020)
- MAF, ICBA. (2012). Oman Salinity Strategy, Annex 1:Assessment of Salinity Problem. Muscat, Sultanate of Oman. 165pp.
- Mehdi S, Ghani S, Khalid M, Sheikh A, Rasheed S, Ajmal M, Ashraf A. 2013. Spatial variability mapping of soil EC in agricultural field of Punjab province (Pakistan) using Geographic Information Techniques. *International Journal of Scientific & Engineering Research*

- 4(11): 325-338.
- Munyati C. (2000). Wetland change detection on the Kafue Flats, Zambia, by classification of a multitemporal remote sensing image dataset. *International Journal of Remote Sensing* 21(9): 1787-1806.
- Omran ESE. (2012). Improving the prediction accuracy of soil mapping through geostatistics. *International Journal of Geosciences* 3(3): 574-590.
- Public Authority of Civil Aviation (PACA). (2020). <http://www.met.gov.om/opencms/export/sites/default/dgman/en/weather-chart/historical-data/index.html> (accessed July 16, 2020)
- Purevdorj T, Tateishi R, Ishiyama T, Honda, Y. (1998). Relationships between percent vegetation cover and vegetation indices. *International Journal of Remote Sensing* 19(18): 3519-3535.
- Rhoades JD, Kandiah A, Mashali AM. (1992). The use of saline waters for crop production. *FAO Irrigation and Drainage Paper 48*. Food and Agriculture Organization of the United Nations. Rome, Italy. 133pp
- Rondeaux G, Steven M, Baret F. (1996). Optimization of soil-adjusted vegetation indices. *Remote Sensing of Environment* 55(2): 95-107.
- Schloeder CA, Zimmerman NE, Jacobs MJ. (2001). Comparison of methods for interpolating soil properties using limited data. *Soil Science Society of America Journal* 65:470-479
- Singh A. (1989). Review article digital change detection techniques using remotely-sensed data. *International Journal of Remote Sensing* 10(6): 989-1003.
- Sommerfeldt T, Rapp E. (1982). Management of saline soils. Canada Department of Agriculture. Ottawa, Ontario. Publication 1642E.
- Tucker C J. (1979). Red and photographic infrared linear combinations for monitoring vegetation. *Remote Sensing of Environment* 8(2): 127-150.
- Walthall C, Dulaney W, Anderson M, Norman J, Fang H, Liang S. (2004). A comparison of empirical and neural network approaches for estimating corn and soybean leaf area index from Landsat ETM+ imagery. *Remote Sensing of Environment* 92(4): 465-474.
- Wiegand C, Rhoades J, Escobar D, Everitt J. (1994). Photographic and videographic observations for determining and mapping the response of cotton to soil salinity. *Remote Sensing of Environment* 49(3): 212-223.
- Xiao Q, McPherson EG. (2005). Tree health mapping with multispectral remote sensing data at UC Davis, California. *Urban Ecosystems* 8(3-4): 349-361.
- Zekri S. (2008). Using economic incentives and regulations to reduce seawater intrusion in the Batinah coastal area of Oman. *Agricultural Water Management* 95(3): 243-252.
- Zhang TT, Zeng SL, Gao Y, Ouyang ZT, Li B, Fang CM, Zhao B. (2011). Using hyperspectral vegetation indices as a proxy to monitor soil salinity. *Ecological Indicators* 11(6): 1552-1562.